Pure & Appl. Chem., Vol. 61, No. 6, pp. 1123–1132, 1989.
Printed in Great Britain.
© 1989 IUPAC

Adiabatic calorimeter as an ultra-low frequency spectrometer*

Hiroshi SUGA and Takasuke MATSUO

Department of Chemistry and Chemical Thermodynamics Laboratory
Faculty of Science, Osaka University, Toyonaka, Osaka 560, Japan

Abstract- High thermal stability and temperature resolution of the adiabatic calorimetry make it possible to study freezing process of disorder existing in condensed matters. This was first demonstrated for liquids around their glass transition regions. It turned out that the enthalpy relaxation phenomenon occurred also in crystalline materials associated with the freezing of relevant degree of freedom. Since the measurement is based on the time evolution of enthalpy through the observation of temperature change under adiabatic condition, the adiabatic calorimetry belongs to time-domain spectroscopy corresponding to the frequency range between 10 mHz and 1 μHz. The method has a feature of applicability to a wide range of substances independently of the chemical nature and physical state. Examples of the frozen-in processes of disorder occurring in several crystals are reviewed here with their implications.

INTRODUCTION

Heat can transfer in various modes; conduction, convection and radiation. This situation gives unique status to the adiabatic calorimetry for the determination of enthalpy change associated with a physical or chemical process (ref. 1). The method minimizes the correction for heat leakage which takes place between a calorimetric cell and surroundings during the measurement and governs primarily the accuracy and precision of the obtained results. Thus the adiabatic calorimetry has been accepted as the most reliable method specifically in determining the heat capacity and related thermodynamic functions of condensed matters at low temperatures. The method played the crucial role in the experimental verification of the third law of thermodynamics (ref. 2).

In a certain number of cases, most notably for H_2O (ref. 3) and CO (ref. 4), the calorimetric entropies were smaller than the spectroscopic entropies. This was the first indication that even these simple substances retain frozen disorder in seemingly thermal equilibrium at low temperatures. Some of the more complex substances such as glycerol (ref. 5) undercool easily without undergoing crystallization down to the lowest temperature. Since the lack of the periodicity of the molecular arrangement is the most clear evidence of the disorder in the non-crystalline state, entropies of liquid as well as vitreous glycerol attracted attention already in 1930. From these studies it was recognized that the frozen state is not a thermodynamic equilibrium state even though it may not undergo perceptible change in the experimental time (ref. 6). Between the high-temperature fluid state and low-temperature solid state, there exists a transitional state called the glass transition region (ref. 7). A typical behavior of the heat capacity in the glass transition region is characterized by a step-like increase of magnitude that differs from one substance to another. At temperatures away from the glass transition the heat capacities are reproducible, while they vary in the glass transition region depending on the sample history.

Some of crystalline substances (cyclohexanol, and some other highly disordered crystals) were also found to exhibit a glass-like behavior (ref. 8). Molecules in these substances form periodic crystal lattices but their orientation relative to the crystal axes is random and aperiodic. The frozen-in disordered states of these crystals are called glassy crystals. Because of the positional and orientational disorder, glassy substances have residual entropies in conjugational way with the glass transitions. It is to be noted that experimental determination of the residual entropy is possible only for the relatively simple substances. Therefore, study of disordered systems based on the determination of the absolute entropy has been limited to those for which the entropy of the frozen state can be related either to the ideal gas state through a chain of accurate experimental data or to a polymorph whose entropy can be determined independently.

* Contribution No. 154 from the Chemical Thermodynamics Laboratory.

CALORIMETRIC SPECTROSCOPY

Vibrational part of the enthalpy of any disordered system always responds quickly to a rapid temperature change. The remaining part of the enthalpy that responds slowly at low temperatures is called the configurational enthalpy. A part of the latter is brought into frozen state due to a prolonged relaxation time. With the development of adiabatic calorimeters which can detect temperature change of sample with the least time lag on one hand and which have a good long-term stability of the adiabatic regulation on the other, it has became possible to study the process, not merely the consequence, of the freezing of the disorder by calorimetry (ref. 9).

Since it is based on the measurement of the time evolution of the enthalpy, or temperature, it belongs to time-domain spectroscopy. Its useful time domain is from 0.1 ks to 0.1 Ms. The short-time limit is set by the thermal time lag in the sample. The long-time limit is dictated by the stability of the thermometry and adiabatic control. Automatic operation of the calorimeters by microcomputers has removed human factors as an agent limiting the operational range of the calorimetric spectrometers.

The calorimetric spectroscopy has several features that distinguish it from other relaxational spectroscopy. Firstly, it measures relaxation of the energy of one form to another in the sample. The heat effect thus determined is directly related to the entropy production that characterizes the irreversible process. Secondly, it is relatively insensitive to spurious effects. When a relaxation is observed by calorimetry, it is a strong evidence that a molecular process involving a fairly large energy is taking place. This may be compared with other types of experiment in which the result depends on the surface effect. Surface electric polarization due e.g. to ionic migration sometimes overshadows the bulk properties we are interested in. Interference due to such spurious effects does not occur in the calorimetric spectroscopy.

PRINCIPLE OF THE EXPERIMENTAL METHOD

Suppose that a sample in a calorimetric cell is placed in an ideal adiabatic condition, so that no heat is exchanged between the sample cell and its environment. When an amount of heat is evolved from the sample, it increases first the sample temperature and then is transmitted to the sample cell where the temperature is measured. The increase of temperature of the sample cell is proportional to the amount of heat that has been evolved. If the thermal conduction between the sample and the cell is sufficiently fast, the measurement of calorimetric temperature as a function of time reproduces the heat evolution rate in the sample. It is important to recognize that the thermometer measures the temperature of itself. In thermal equilibrium, the temperatures of the thermometer, sample cell and sample are all equal. But they are different in general when the temperature varies in time. If the rate of heat evolution from the sample is sufficiently small, then the thermometer, sample cell and the fast-responding vibrational degrees of freedom of the sample are at the same temperature. They are represented by a heat capacity as a whole that supplies or receives thermal energy to and from the configurational degree of freedom of the sample.

Since the heat evolution experiment is made under an adiabatic condition rather than isothermal, temperature dependence of the relaxational property of the sample has to be taken into account. Let H_c^{ex} represent the excess configurational enthalpy over that of the equilibrium value. It is a function of temperature T, time t and a time constant τ characterizing the relaxational property of the configurational enthalpy for a given initial state. Its temperature dependence enters through the temperature dependence of the equilibrium enthalpy.

$$H_c^{ex} = H_c^{ex}(T, t, \tau). \tag{1}$$

In the adiabatic condition, enthalpy of the whole calorimetric system is constant with time.

$$H_c^{ex} + H_o = \text{constant}, \tag{2}$$

where H_o represents the sum of the enthalpy of the sample cell and the fast-responding part of the sample enthalpy. Differentiation of both sides with time gives

$$\frac{dH_c^{ex}}{dt} = -\frac{dH_o}{dt}. \tag{3}$$

With the assumption that the variation of temperature is sufficiently slow to ensure that the fast-responding part of the sample and the cell with its thermometer and heater are

represented by a single temperature, the RHS of eq. (3) may be written as follows

$$\frac{dH_o}{dt} = \frac{dH_o}{dT}\frac{dT}{dt} \tag{4}$$

$$= C_o \frac{dT}{dt} \tag{5}$$

where C_o is the heat capacity corresponding to H_o. Hence

$$\frac{dH_c^{ex}}{dt} = -C_o \frac{dT}{dt} \tag{6}$$

This equation relates the configurational enthalpy to the experimentally accessible quantities. Relation between dH_c^{ex}/dt and the isothermal relaxation rate $(\partial H_c^{ex}/\partial t)_{T,\tau}$ is given as follows

$$\frac{dH_c^{ex}}{dt} = \left(\frac{\partial H_c^{ex}}{\partial t}\right)_{T,\tau} + \left(\frac{\partial H_c^{ex}}{\partial T}\right)_{\tau,t}\frac{dT}{dt} + \left(\frac{\partial H_c^{ex}}{\partial \tau}\right)_{\tau,t}\frac{d\tau}{dt}$$

$$= \left(\frac{\partial H_c^{ex}}{\partial t}\right)_{T,\tau} + \left(\frac{\partial H_c^{ex}}{\partial T}\right)_{\tau,t}\frac{dT}{dt} + \left(\frac{\partial H_c^{ex}}{\partial \tau}\right)_{T,t}\frac{d\tau}{dT}\frac{dT}{dt} \tag{7}$$

The first term on the right is the isothermal relaxation rate which is more easy to analyse and which we would like to determine experimentally. The second term shows the effect of the temperature dependence of H_c^{ex} through the temperature dependence of the equilibrium configurational enthalpy as stated above. The third term represents the effect of the changing temperature, as the relaxation proceeds, on the relaxation rate via the temperature dependence of τ. The second and third correction terms depend on the details of the substance being studied and specific conditions of the experiment. They are usually small and often neglected.

Two types of experiments are possible. In the first, the sample is cooled rapidly from a high temperature where the whole thermal equilibrium is reached in a short time to the temperature at which one wants to study the relaxation. The calorimetric system is then kept under the adiabatic control. As the relaxation proceeds in the sample, the calorimetric temperature rises gradually. The temperature versus time data can be identified with the excess configurational enthalpy versus time data if the zero of the two quantities are suitably chosen. The curve is then analysed by comparing with appropriately parametrized functional forms, taking the correction terms in eq. 7 into account if necessary. By varying the initial temperature stepwise, one obtains a series of relaxational data at different temperatures.

In the second type of experiment, one obtains the temperature dependence of the relaxational property from a single quenching. First the sample is quenched from a high temperature to a sufficiently low temperature where the relaxation time is long enough to ensure that no appreciable relaxation takes place in the course of the first few heat capacity determinations. The heat capacity is measured as in ordinary adiabatic method, by increase the temperature by a few Kelvin in one determination of C_p. As the glass transition temperature is approached, exothermic temperature drift appears in the equilibration period. The temperature drifts are measured for a fixed time, e.g. 1 ks in each equilibration. At the lower temperature where the relaxation time is much longer than this, the temperature drifts are in effect linear in time, the slope being proportional to the heat evolution rate. As the heat capacity measurement enters the glass transition region, the linear drift rate increases at first, reaches a maximum and then decreases fast, crossing the zero to become negative (endothermic) and finally non-linear in time. The maximum of the drift rate occurs as the compromise of the increasing relaxation time and decreasing excess configurational enthalpy, as the temperature is raised. Data obtained in this type of experiment can be analysed on a simplifying assumption that the relaxational rate is proportional to the excess enthalpy,

$$C_o \frac{dT}{dt} = \frac{H_c^{ex}}{\tau} \quad , \tag{8}$$

from which one obtains the relaxation time τ as follows

$$\tau = \frac{H_c^{ex}(T,t)}{C_o(dT/dt)} \quad , \tag{9}$$

$$H_c^{ex}(t) = H_c^{ex}(o)\ \exp\ (-t/\tau) \tag{10}$$

The quantity $H_c^{ex}(T,t)$ is the excess configurational enthalpy at temperature T and time t at which the drift rate is determined. This is given by successive backward addition of the quantities

$$-\Delta_n H_c^{ex} = C_o \int_{t_1}^{t_2} (\frac{dT}{dt})_n dt \ , \tag{11}$$

where t_1 and t_2 are the mid-times of the heating period previous and subsequent to the n-th drift measurement, respectively. The zero of H_c^{ex} corresponds to the zero drift rate that occurs at the crossing of the actual and equilibrium enthalpy curves.

The assumption eq. 8 greatly simplifies the analysis of the experimental data but may be appropriate only for a limited group of substances, of which an example will be given below. For other group of substances it may be replaced by more complicated relaxation laws such as the Kohlrausch-Williams-Watts function (ref. 10),

$$H_c^{ex}(t) = H_c^{ex}(o)\exp[-(t/\tau)^{\beta}] \ . \tag{12}$$

However, this entails less straightforward interpretation of the result of the analysis.

EXPERIMENTAL APPARATUS

A cross-sectional view of typical adiabatic calorimeter used for the ultra-low frequency spectroscopy is shown in Fig. 1. It consists of the sample cell, two adiabatic shields, thermal anchor, liquid hydrogen tank and liquid nitrogen dewar. The outer shield, kept always a few Kelvin lower than that of the calorimetric cell, allows to make finer control of the inner adiabatic shield. The sample cell is shown in a larger scale in Fig. 2. It is a double walled cylindrical copper container, 16 mm in the inner diameter and 25 mm in the length. The thermometer (nominal 100 Ω at 273 K, 3.2 mm in diameter and 13 mm long) is placed in a close fitting copper tube and tightly fixed on the cover of the cell with screws. The thermal contact between the thermometer unit and the cell is an important factor in the design of the cell. If the thermal contact is poor, the thermometer does not follow the temperature of the main body of the cell. The two screws were found satisfactory to secure the good thermal contact between the thermometer unit and the top of the cell, whereas thermal contact between the thermometer and the unit is achieved by the snug fitting between them and facilitated by a piece of gold foil that fills any remaining gap. An effect of the thermal resistance in question here is that the thermometric temperature lags behind the main body of the cell when the latter is heated. Magnitude of this lag is such that the temperature indicated by the thermometer continues to increase for a while and becomes constant to ±0.1 mK within *ca* 20 s after heating. Thermal conduction between the cell and the sample (often crystalline powder) can be a more restricting difficulty. The best we can do is to provide fins in the cell to reduce the thermal path length in the sample. It is also essential to fill the dead space in the cell with helium gas. An effect of the thermal lag of the sample behind the cell is that the thermometric temperature decreases for a while after heating, as a quantity of heat is transferred from the cell and thermometer to the sample while they are adiabatically isolated as a whole. An example of this effect is given later in which the temperature becomes uniform within 100 s after heating. In former times, we experienced much larger decrease of temperature after heating.

Two factors appear to contribute to the improved situation. First, the volume of the cell was typically 25 cm^3 in the former time as compared 4.6 cm^3 shown in Fig. 2. This allows smaller heating power to be used to achieve the same heating rate, resulting in smaller local heating within the cell. The second point is that the heating wire covers a large part of the surface area of the cell in the recent design. This results in even generation of the Joule heat in the cell and gives a shorter equilibration time. In the typical former design, the heating wire was often localized around the thermometer. This was harmless and even reasonable when spectroscopic use of the calorimeter was not intended. For the present purpose, it is important that the thermometer indicates the sample temperature which may change in time. The apparent temperature change caused by the redistribution of the Joule heat generated at the heater should be as small as possible within a reasonable degree of design complication.

Another point which is often overlooked and becomes important for small sample cell is the thermal lag of the thermocouple wires straddled between the cell surface and the adiabatic shield. Since the thermocouple wires have a small non-vanishing heat capacity, a quantity of heat has to be supplied to them when the sample is heated. This is achieved by the thermal conduction along the wires themselves. Since thermocouple wires are usually alloy of poor thermal conductivity, it takes some time for this process. This cannot be negligible for small cell, especially if teflon cover is used for the insulation of the wires. This effect may be minimized by the use of thin (and short) thermocouple wires covered with insulating material as thin as is practical.

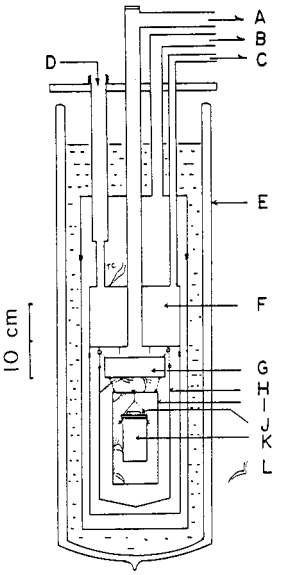

A: Evacuation(inner)
B: Evacuation(outer)
C: Hydrogen gas outlet
D: Liquid hydrogen inlet
E: Liquid nitrogen dewar
F: Liquid hydrogen tank
G: Thermal anchor
H: Outer adiabatic shield
I: Inner adiabatic shield
J: Thermometer
K: Sample cell
L: Thermocouples

Fig. 1 Cross-section of the cryostat

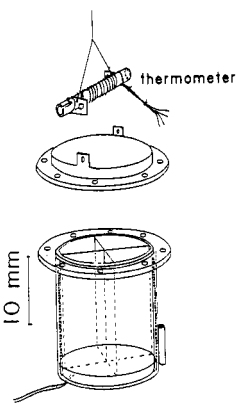

Fig. 2 Sample cell

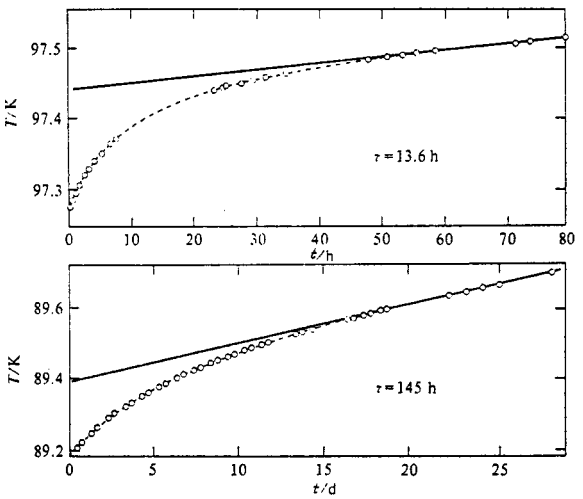

Fig. 3 Typical runs of enthalpy relaxation experiments of pure ice.

EXPERIMENTAL RESULTS

Freezing process occurs not only in undercooled metastable phase but also in stable phase. Typical example is hexagonal ice which has been known as the most stable modification of ice under atmospheric pressure. In the course of remeasurement of heat capacity, we have encountered enthalpy relaxation occurring slowly around 100 K (ref. 11). Typical two examples of the first-type relaxation experiments on pure ice crystal are reproduced in Fig. 3. The sample cell was cooled with a rate of 1 K min^{-1} from 120 K at which the thermal equilibrium could be reached quickly. The calorimetric temperature rises exponentially at the initial stage and approaches a stationary drift rate at the final stage of each relaxation experiment. The observation at 89 K was the longest relaxation experiment we have done so far. The initial exponential rise of temperature is considered to be due to a slight tendency towards a more ordered arrangement of proton configuration in the lattice. The configurational enthalpy relaxes towards the equilibrium value very slowly at 89 K, but the relaxation time becomes shorter and shorter as the temperature is raised. The straight part of the temperature change arises from residual heat leakage. By changing stepwise the initial temperature, a series of relaxation time data were obtained.

In a separate second-type relaxation experiment, a small heat-capacity jump and the associated exothermic followed by endothermic temperature drifts were observed. The annealed samples used in the first-type experiments showed increasing heat-capacity jumps in the subsequent heat capacity measurements. These are typical behaviors of vitreous liquids around their glass transition regions. Ice was already known to have a residual entropy (ref. 3) which was explained in terms of completely disordered pattern of proton location under the ice conditions (ref. 12). Ice was not an exceptional case of the glassy crystals. The ice conditions constraint severely the rearrangement of proton configuration or reorientational motion of water molecules in the lattice, leading to freezing of that degree of freedom around 100 K. This possibility has been conjectured already from dielectric measurement (ref. 13).

A trace amount of alkali hydroxides incorporated into the ice lattice was found to shorten dramatically the relaxation time for the water reorientation (ref. 14). An ice specimen doped with KOH in mole fraction x of 1.8×10^{-3} exhibited a first-order phase transition at 72 K (ref. 15). The specimen was annealed at 65 K in advance for a few days for a complete transformation into the low temperature phase. The transition removed the substantial fraction of the residual entropy and the proton-ordered ice was designated as ice XI (ref. 16) (orthorhombic system as determined by a neutron diffraction experiment (ref. 17)). Thus the dopants have significant effect to remove the kinetic hindrance and to reveal the equilibrium configurational heat capacity of ice within a reasonable time.

Lithium hydroxide also exhibits the catalytic action for the acceleration of the water reorientation (ref. 18). The excess part of the heat capacity due to the configurational degree of freedom is drawn in Fig. 4. It is interesting to note that the LiOH(x=1.8 x 10^{-3})-doped ice specimen shows undercooling of hexagonal phase with the development of increasing short-range order down to 60 K, where the freezing hinders the crystal to reach a hypothetical ordering transition in the hexagonal phase. The freezing temperature shifted from 100 K to 60 K by the doping. On annealing the doped specimen around 65 K for five days, it transformed into the ordered phase. It is intriguing to infer the possible structures of proton ordered arrangement in the undercooled phase keeping the hexagonal symmetry. This problem has been discussed once by Bernal and Fowler (ref. 19) and the suggested space group was C_{6v}^3 - C6mc with z= 12.

Thiophene is a unique crystal in which freezing process occurs in both of stable and metastable phases. Thiophene has been found to exhibit five modifications (I, II, III, IV and V from the high temperature side) in the first calorimetric measurement (ref. 20). Later, the phase II was found to undercool easily to give a metastable phase sequence; II_1 and II_2. The phase sequence is summarized as follows:

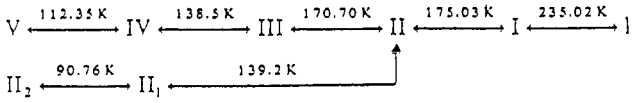

Metastable-phase sequence

Our remeasurement of heat capacity for each phase sequence showed that both of the lowest-temperature phase, V and II_2, exhibited small heat-capacity jumps and anomalous temperature drifts, respectively (ref. 21). The experimental results are shown in Fig. 5(a) and 5(b). This is the results obtained by the second-type relaxation experiments. Careful comparison of the calorimetric entropies with spectroscopic entropy showed that both the lowest-temperature phases retain their residual entropies which surmount the experimental uncertainty (ref. 22). Already a dielectric study of thiophene crystal revealed the existence of dielectric dispersion at temperature as low as 80 K when measured at 30 kHz (ref. 23). There was no description in the report as to whether the measurement was done on phase V or II_2. Because they were not aware of existence of the metastable phase sequence at that time. As given in Fig. 6, a comparison of the relaxation time data derived from the calorimetric and dielectric measurements showed that the dielectric study was possibly done on phase II_2, the metastable phase. Owing to the long extrapolation of the data, however, careful dielectric measurements with lower frequencies on well-characterized phase are highly desirable. Close correlation between the calorimetric and dielectric relaxation times will be discussed later.

The study of reorientational and collective ordering processes of linear cyanide ions in alkali cyanide crystals is a field of intense current interest (ref. 24). This is because of the cubic symmetry of the lattice at room temperature and the simple dumb-bell shape of the cyanide ion. A large amount of work has been spent on the structure and lattice dynamics. For example, pure KCN crystal undergoes a first-order phase transition at 168 K (ref. 25) from the NaCl-type cubic (I) to an orthorhombic low-temperature phase (II), accompanied by a strong softening of the shear elastic constant c_{44} (ref. 26). Hence, the name "elastic" is given to this phase transition. On further cooling, a λ-type transition arising from head-to-tail ordering of the CN^- ions appears at 83 K (ref. 25). The transition is driven by electric dipole-dipole interaction of the CN^- ions (ref. 27), giving rise to an antiferroelectrically ordered orthorhombic phase (III). Therefore, the name "electric" is given to the second transition. NaCN crystal also exhibits the same trimorphism (ref. 28).

For RbCN crystal, the elastic transition occurs at 132 K (ref. 29). The low temperature phase belongs to the monoclinic system and the head-to-tail disorder of the CN^- ions persists in this phase, as evidenced by calorimetry (ref. 30), dielectric measurement (ref. 31) and neutron diffraction (ref. 32). Transition temperature plotted as a function of interanionic distance $d(CN^- - CN^-)$ is given in Fig. 7 (ref. 24). The estimated temperature for a hypothetical electric transition in RbCN is very low, indicating a possibility of freezing out of the head-to-tail reorientational motion of the CN^- ions before the crystal arrives at the electrically ordered phase. Actually we found a relaxational heat-capacity anomaly in RbCN crystal around 30 K (ref. 33). The experimental heat capacity data are given in Fig. 8. Typical four runs of the spontaneous temperature change observed in the second-type relaxation experiment are given in Fig. 9. The enthalpy relaxation rate, measured as the spontaneous temperature drift rate, was described with a function consisting of terms exponential and linear in time, each describing the relaxation part and heat leakage. The best-fit parameters were determined by the least-squares method, and the fitting is shown in the figure by curves A to D. The first curve shows an exothermic relaxation, the second and third endothermic relaxation, and the fourth normal behavior. The relaxation time values thus determined are shown in Fig. 10 together with those obtained earlier by dielectric (ref. 31) and ionic thermal current (ref. 34) measurements. All the data can be connected smoothly by a single straight line, indicating that all the relaxation effects have a common physical origin. It is interesting to note that all the relaxation time data including those of NMR method (ref. 35) (which are not shown in the figure) follow a single Arrhenius equation covering $\tau(T)$ over 12 decades from ns to ks.

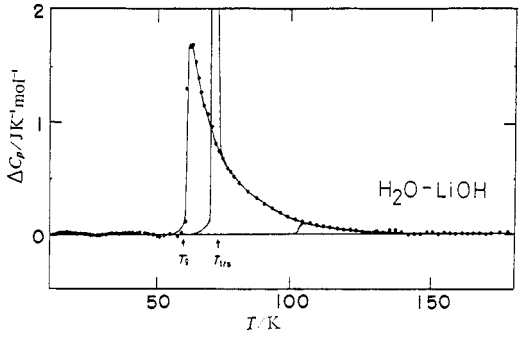

Fig. 4 Excess heat capacity due to transitions of LiOH-doped ice crystals

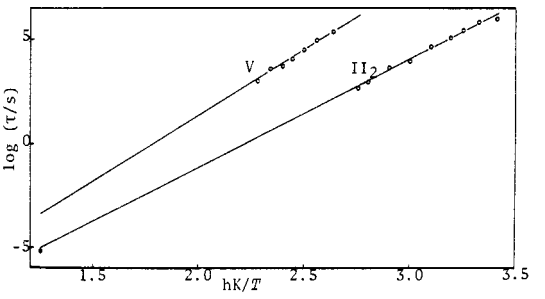

Fig. 6 Comparison of calorimetric(o) and dielectric(●) relaxation time data of thiophene crystal

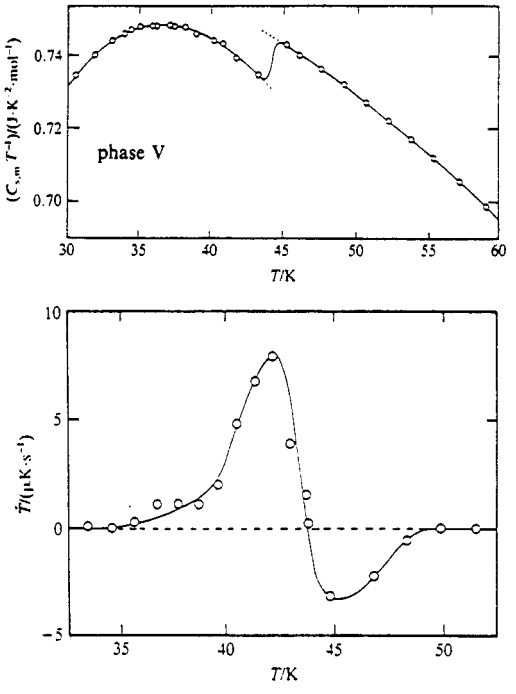

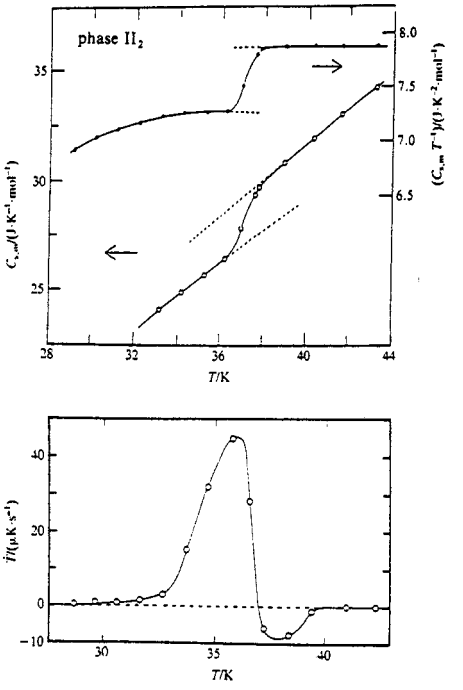

Fig. 5 Glass transition of thiophene in phase V (left a) and phase II_2 (right b)

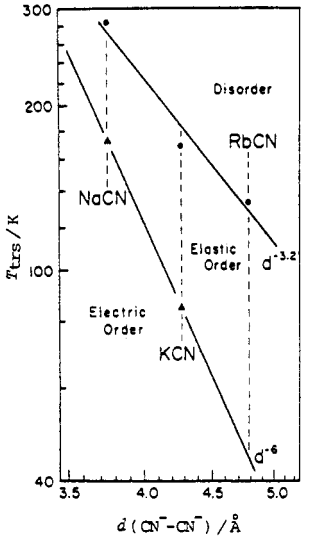

Fig. 7 Transition temperatures of some alkali cyanides

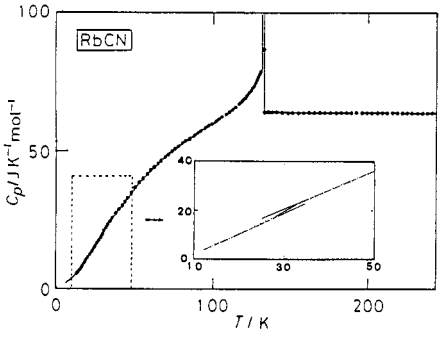

Fig. 8 Heat capacity of RbCN crystal

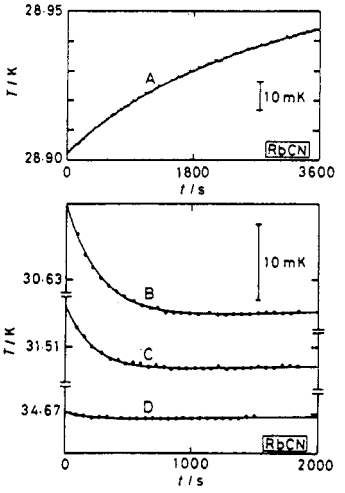

Fig. 9 Typical runs of enthalpy relaxation in RbCN crystal

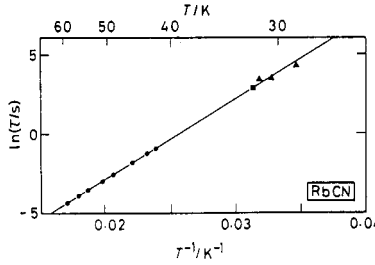

Fig. 10
Relaxation time data for reorientational motion of CN^- ions in RbCN obtained by dielectric(●), ionic thermal current(■), and calorimetric (▲) measurements

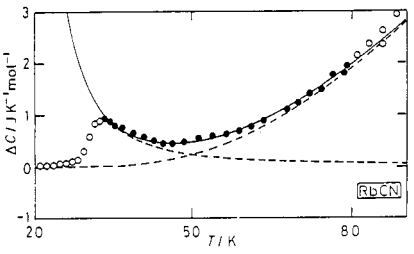

Fig. 11
Excess heat capacity of RbCN due to glass transition and phase transition. The broken lines represent the high-temperature approximation for the glass transition and the low-temperature approximation for the phase transition, both being based on the s 1/2 Ising model and on the fcc lattice

$S = 1/2$ Ising model of the face-centered-cubic lattice

$T > T_c$

$w = \tanh(J_1/RT)$

$C/R = (J_1/RT)^2(6 + 48w + 390w^2 + 3216w^3 + 26\,844w^4 + 229\,584w^5)$

$T < T_c$

$u = \exp(-4J_2/RT)$

$C/R = (J_2/RT)^2(576u^6 + 11\,616u^{11} - 14\,976u^{12} + 28\,800u^{15} + 172\,032u^{16})$

The heat capacities below 30 K are free from the slow-relaxing part which originates from the configurational enthalpy of the CN^- ions. The normal heat capacity was assumed to be represented by a combination of Debye and Einstein functions whose characteristic temperatures were determined by the least-squares fit of the model heat-capacity function to the experimental data below 30 K. A part of the excess heat capacity arising from the configurational degree of freedom is drawn in Fig. 11. The elastic transition reveals its shape entirely but the electric transition partly, only the high-temperature tail of its shape due to the kinetic hindrance. In order to understand the reason why the CN^- ions freeze in its paraelectric state in RbCN while they become ordered electrically in NaCN and KCN, both the kinetic and equilibrium aspects of the problem need to be considered.

The head-to-tail reorientational problem of the CN^- ions has an analogy of the Ising spin system with $s = 1/2$ (up and down). This situation makes to replace the electric transition of the CN^- ions with magnetic transition of the Ising system. Series expansion expression of heat capacity for the $s = 1/2$ Ising system of the fcc lattice (ref. 36) can be used as a model function to be fitted to the experimental heat capacity data between T_g and the elastic transition temperature. The expression for $T < T_c$ should be used for the low temperature tail of the elastic transition and that for $T > T_c$ for the high temperature tail of the electric transition. J_1 is an interaction parameter characterizing the electric transition and J_2 the elastic transition. The calculated heat capacity and its decomposition into the two contributions are plotted in the figure together with the experimental data. The best-fit value of J_1 parameter is 20.8 J mol^{-1}, which can be correlated immediately to the hypothetical transition temperature, 24.5 K. This is the temperature at which dipolar ordering would take place in an equilibrium experiment for RbCN.

Extrapolation of the dielectric relaxation time in the Arrhenius plot to low temperature gives the relaxation time $\tau = 4.56$ Ms= 53 days at 24.5 K. This is substantially longer than the usual experimental time. Naturally we could not obtain the electrically ordered phase of RbCN. The excess entropy associated with the glass transition is 0.33 J K^{-1} mol^{-1} compared with $R \ln 2 = 5.76$ J K^{-1} mol^{-1} which we could have obtained if we started from the completely ordered state at the lowest temperature. The difference between the two values is the residual entropy 5.43 J K^{-1} mol^{-1}. This quantity corresponds to the development of short-range order by 4 % from the complete disorder. According to neutron diffraction experiment, the carbon and nitrogen occupancy factors are (0.50±0.05), respectively. The week short-range order derived here from the calorimetric measurement may be detected by neutron scattering experiment. Electric dipolar interaction is strongly angle dependent. In the paraelectric state, all of the CN^- dipoles are parallel in NaCN and KCN. By contrast they are at skewed orientations close to perpendicular along a particular axis in RbCN. This structural difference may be responsible for the small value of the interaction parameter J_1 and hence for the low transition temperature that leads to their frozen disorder.

Similar problem arises in KCN-KBr binary system. These mixed crystals belong to the well-known family of mixed cyanide crystals such as $Rb(CN)_xBr_{1-x}$, $K_xRb_{1-x}CN$ (ref. 37), which exhibit rich and interesting phase diagram. A tentative phase diagram of $K(CN)_xBr_{1-x}$ mixed crystal was given by Loidl *et. al* (ref. 38) and reproduced in Fig. 12 with slight modifications. The mixed crystals in the region $x \sim 1.0$ is trimorphic, undergoing their elastic and electric transitions, respectively. For $0.6 < x < 0.9$, the cubic phase transforms into a monoclinic phase, which also appears as a metastable phase in pure KCN by a special thermal cycling (ref. 39). The partial substitution of CN^- by Br^- ions leads to stabilization of the monoclinic form due to random local strain in the lattice (ref. 40). In the stability reversal region, a mixture of the monoclinic and orthorhombic modifications is produced. The substitution leads to reduction of the transition temperatures and eventually the crystal remains cubic down to the lowest temperature. For the concentration $0.6 < x < 0.9$, the monoclinic phase is elastically ordered but electrically disordered. It is interesting to examine again what happens to the head-to-tail orientational degree of freedom of the CN^- ions in this phase.

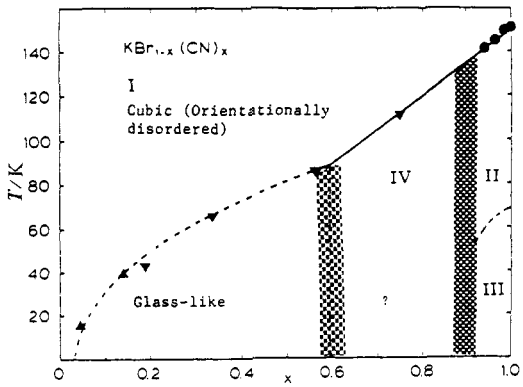

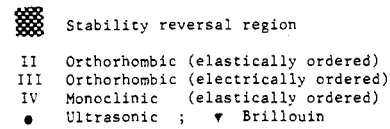

Fig. 12 Phase diagram of KBr-KCN binary system

Figure 13 shows the heat capacity data of $K(CN)_{0.7}Br_{0.3}$ mixed crystal (ref. 41). The broad peak at 112 K is due to the elastic transition which occurs much sharply in pure KCN and RbCN. A relaxational behavior was observed between 20 and 30 K. Typical result of spontaneous temperature rise of the calorimetric cell observed at 25 K after it had been cooled from 40 K is drawn in Fig. 14. It had been tested in previous measurements that the thermal equilibrium of the calorimetric cell was established within 60 s at 40 K. The time scale involved in the relaxation is much longer than the time constant of the calorimeter, showing that the relaxation is definitely a genuine property of the mixed crystal. Careful analysis showed that the slow-relaxing part could not be reproduced by an exponential function with a single relaxation time. This non-exponential behavior is familiar in the relaxation processes of many physical quantities around the glass transition region of organic and inorganic glasses of monomeric and polymeric nature (ref. 42). The behavior was found to be reproduced in terms of the Kohlrausch-Williams-Watts relaxation function. The function was modified in the following form so as to reproduce the present experimental data.

$$T(t) = A + Bt - C \exp\left[-(t/\tau)^{\beta}\right] , \qquad (13)$$

where $T(t)$ is the temperature at time t, $(A-C)$ the initial temperature, B the constant drift rate due to residual heat leakage, C the amplitude of the relaxation, τ the relaxation time and β the K-W-W parameter. The full line in the figure is the best-fitting model function with parameters $\beta = 0.62$ and $\tau = 6.0$ ks. This result with those obtained for other temperatures show that the relaxation in this simple glassy crystal can be described by the K-W-W function with parameter values that are common in structurally more complicated glassy liquids. This is the first application of the K-W-W function to the relaxation in crystalline substance. The deviation of β from unity can be most simply related with wide distribution of relaxation time in the system (ref. 42). The CN^- ions are considered to be located in various environments with respect to the reorientational motion in the mixed crystal, leading to the non-uniform relaxations for the motion.

Similarity of the present mixed crystal to pure RbCN is briefly mentioned. Both are monoclinic system and disordered with respect to the orientation of the CN^- ions. RbCN crystal undergoes a distinct glass transition at 30 K in the calorimetry. But the mixed crystal does not show a clear heat-capacity jump in the ordinary measurement. However, the long-time data plotted in the figure gave slightly larger heat capacity than the ordinary measurement. The excess configurational heat capacity is 0.12 J K^{-1} mol^{-1} at 24.1 K and 0.06 J K^{-1} mol^{-1} at 26.1 K. These quantities are too small to estimate the hypothetical temperature for the electric transition. The very much smeared-out glass transition may be a characteristic of the mixed system. Both crystals are a kind of dipolar glasses. At the moment we have no means or way by which the relaxation times for the reorientational motion are shortened so as to reveal the entire shape of the equilibrium configurational heat capacity, as in the case of hexagonal ice.

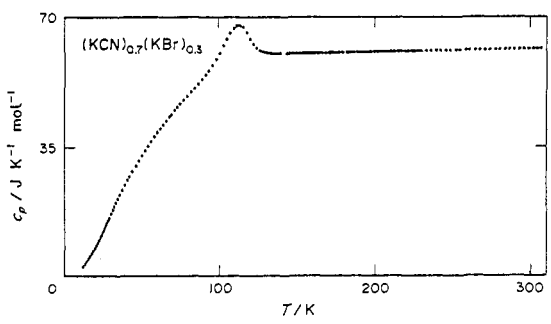

Fig. 13 Heat capacity of $KBr_{0.3}(CN)_{0.7}$ mixed crystal

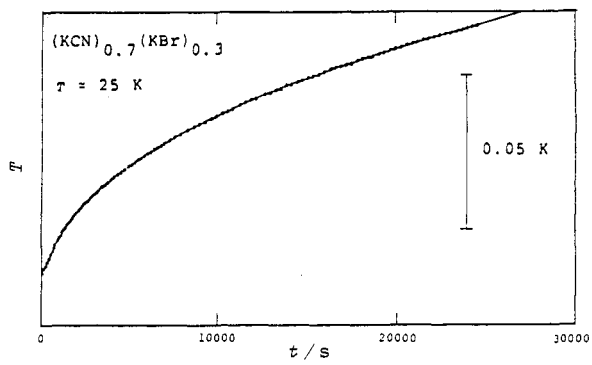

Fig. 14 Enthalpy relaxation of $KBr_{0.3}(CN)_{0.7}$ observed at 25 K

CONCLUDING REMARKS

In this way the adiabatic calorimetry found a novel role as an ultra-low frequency spectrometer in the range between mHz and uHz in addition to the traditional mission. The time domain less than hs would be reached by the present method only after a drastic modification of the apparatus, which has not been attempted thus far. The method has a feature of applicability to a wide range of substance independently of the chemical nature, such as polarity, of the molecules and physical state (liquid, solid or powder) of the sample using the same apparatus. Only requirement on the sample is that the relaxational motion of molecules contributes a measurable magnitude of enthalpy to the total sample enthalpy and that the relaxation time depends on temperature fairly strongly. Careful experiments with highly-sensitive and highly-stabilized adiabatic calorimeter will prove the wide occurrence of freezing processes in condensed matters with respect to positional, orientational, conformational, or magnetic degree of freedom.

Acknowledgement The authors would like to express their hearty thanks to many collaborators and colleagues who have joined the actual experiments reviewed partly here.

REFERENCES

1. J. P. McCullough and D. W. Scott ed., *Experimental Thermodynamics, Vol. 1. Calorimetry of Non-reacting Systems*, Butterworths, London (1967).
2. N. G. Parsonage and L. A. K. Staveley, *Disorder in Crystals*, Clarendon Press, Oxford (1978).
3. J. W. Stout and W. F. Giauque, *J. Am. Chem. Soc.* 58, 1144 (1936).
4. J. O. Clayton and W. F. Giauque, *J. Am. Chem. Soc.* 54, 2610 (1932).
5. F. E. Simon, *Z. Anorg. Allg. Chem.* 203, 219 (1931).
6. W. Kauzmann, *Chem. Rev.* 43, 219 (1948).
7. R. Zallen, *The Physics of Amorphous Solids*, John Wiley and Sons' Inc., New York (1983).
8. H. Suga and S. Seki, *J. Non-cryst. Solids* 16, 171 (1974).
9. H. Suga and S. Seki, *Faraday Discussion*, Roy. Soc. Chem. No. 69, 221 (1981); T. Matsuo and H. Suga, *Thermochim. Acta* 88, 149 (1985).
10. G. Williams and D. C. Watts, *Trans. Faraday Soc.* 66, 80 (1970).
11. O. Haida, T. Matsuo, H. Suga and S. Seki, *J. Chem. Thermodyn.* 6, 815 (1974).
12. L. Pauling, *J. Am. Chem. Soc.* 57, 2680 (1935).
13. W. Kauzmann, *Rev. Mod. Phys.* 14, 12 (1942).
14. M. Ida, N. Nakatani, K. Imai and S. Kawada, *Sci, Rep. Kanazawa Univ.* 11, 13 (1966); S. Kawada, *J. Phys. Soc. Jpn.* 44, 1881 (1978).
15. Y. Tajima, T. Matsuo and H. Suga, *Nature* 299, 810 (1982).
16. T. Matsuo, Y. Tajima and H. Suga, *J. Phys. Chem. Solids* 47, 165 (1986).
17. A. Leadbetter, R. C. Ward, J. W. Clark, P. A. Tucker, T. Matsuo and H. Suga, *J. Chem. Phys.* 82, 424 (1985).
18. Y. Miyazaki, T. Matsuo and H. Suga, to be published.
19. J. D. Bernal and R. H. Fowler, *J. Chem. Phys.* 1, 515 (1933).
20. G. Waddington, J. W. Knowlton, D. W. Scott, G. D. Oliver, S. S. Todd, W. N. Hubbard, J. C. Smith and H. M. Huffman, *J. Am. Chem. Soc.* 71, 797 (1949).
21. P. Figuière, H. Szwarc, M. Oguni and H. Suga, *J. Phys. Lett.* 45, L-1167 (1984).
22. P. Figuière, H. Szwarc, M. Oguni and H. Suga, *J. Chem. Thermodyn.* 17, 949 (1985).
23. M. Matsumoto and S. Kondo, *Nippon Kagaku Zasshi (J. Chem. Soc. Jpn.)* 83, 261 (1962).
24. F. Luty, in *"Defects in Insulating Crystals"* ed. V. M. Tuchkevich and K. K. Shvarts, pp. 69, Springer-Verlag, Berlin (1981).
25. H. Suga, T. Matsuo and S. Seki, *Bull. Chem. Soc. Jpn.* 41, 1115 (1965).
26. S. Haussühl, *Solid State Commun.* 13, 147 (1973).
27. B. Koiller, M. A. Davidovich, L. C. Scavarda do Carmo and F. Luty, *Phys. Rev.* B29, 3586 (1984).
28. T. Matsuo, H. Suga and S. Seki, *Bull. Chem. Soc. Jpn.* 41, 583 (1968).
29. Y. Kondo, D. Schoemaker and F. Luty, *Phys. Rev.* B19, 4210 (1979).
30. M. Sugisaki, T. Matsuo, H. Suga and S. Seki, *Bull. Chem. Soc. Jpn.* 41, 1748 (1968).
31. F. Luty and J. Ortiz-Lopez, *Phys. Rev. Lett.* 50, 1289 (1983).
32. J. M. Rowe, J. J. Rush and F. Luty, *Phys. Rev.* B29, 2168 (1984).
33. T. Shimada, T. Matsuo, H. Suga and F. Luty, *J. Chem. Phys.* 85, 3530 (1986).
34. M. Siu Li and F. Luty, *Bull. Am. Phys. Soc.* 28, 385 (1983).
35. W. Buchheit, S. Elschmer, H. D. Maier, J. Petersson and E. Schneider, *Solid State Commun.* 38, 665 (1981).
36. C. Domb, *Adv. Phys.* 9, 149 (1960); G. A. Baker, Jr., *Phys. Rev.* 129, 99 (1963).
37. A. Loidl, T. Schräder, R. Böhmer, K. Knorr, J. K. Kjem and R. Born, *Phys. Rev.* B34, 1238 (1986).
38. A. Loidl, R. Feile and K. Knorr, *Z. Phys.* B42, 143 (1981).
39. G. S. Parry, *Acta Cryst.* 15, 601 (1962).
40. J. M. Rowe, J. Bouillot, J. J. Rush and F. Luty, *Physica* 136B, 498 (1986).
41. T. Matsuo, I. Kishimoto, H. Suga and F. Luty, *Solid State Commun.* 58, 177 (1986).
42. S. Brawer, *Relaxation in Viscous Liquids and Glasses*, Am. Ceram. Soc., Columbus, Ohio (1985).